

Review Article

Novel Applications of Ferrites

Raúl Valenzuela

*Departamento de Materiales Metálicos y Cerámicos, Instituto de Investigaciones en Materiales,
Universidad Nacional Autónoma de México, P.O. Box 70360, Coyoacán 04510, México City, DF, Mexico*

Correspondence should be addressed to Raúl Valenzuela, raulvale@yahoo.com

Received 26 July 2011; Accepted 21 December 2011

Academic Editor: Arcady Zhukov

Copyright © 2012 Raúl Valenzuela. This is an open access article distributed under the Creative Commons Attribution License, which permits unrestricted use, distribution, and reproduction in any medium, provided the original work is properly cited.

The applications of ferrimagnetic oxides, or ferrites, in the last 10 years are reviewed, including thin films and nanoparticles. The general features of the three basic crystal systems and their magnetic structures are briefly discussed, followed by the most interesting applications in electronic circuits as inductors, in high-frequency systems, in power delivering devices, in electromagnetic interference suppression, and in biotechnology. As the field is considerably large, an effort has been made to include the original references discussing each particular application on a more detailed manner.

1. Introduction

Ferrites are a large class of oxides with remarkable magnetic properties, which have been investigated and applied during the last ~50 years [1]. Their applications encompass an impressive range extending from millimeter wave integrated circuitry to power handling, simple permanent magnets, and magnetic recording. These applications are based upon the very basic properties of ferrites: a significant saturation magnetization, a high electrical resistivity, low electrical losses, and a very good chemical stability. Ferrites can be obtained in three different crystal systems by many methods, and the feasibility to prepare a virtually unlimited number of solid solutions opens the means to tailor their properties for many applications. For many applications, ferrites cannot be substituted by ferromagnetic metals; for other, ferrites often compete with metals on economic reasons.

The possibility of preparing ferrites in the form of nanoparticles has open a new and exciting research field, with revolutionary applications not only in the electronic technology but also in the field of biotechnology.

In this paper, the applications of ferrites developed in the last 10 years are briefly described.

2. Ferrites

2.1. Spinel. Spinel ferrites possess the crystal structure of the natural spinel MgAl_2O_4 , first determined by Bragg [2]. This

structure is particularly stable, since there is an extremely large variety of oxides which adopt it, fulfilling the conditions of overall cation-to-anion ratio of 3/4, a total cation valency of 8, and relatively small cation radii. Spinel structure is shown in Figure 1. Cation valency combinations known are 2, 3 (as in $\text{Ni}^{2+}\text{Fe}_2^{3+}\text{O}_4$); 2, 4 (as in Co_2GeO_4); 1, 3, 4 (as in LiFeTiO_4); 1, 3 (as in $\text{Li}_{0.5}\text{Fe}_{2.5}\text{O}_4$); 1, 2, 5 (as in LiNiVO_4); 1, 6 (as in Na_2WO_4). In ferrites with applications as magnetic materials, Al^{3+} has usually been substituted by Fe^{3+} . An important ferrite is magnetite, $\text{Fe}^{2+}\text{Fe}_2^{3+}\text{O}_4$ (typically referred as Fe_3O_4), probably the oldest magnetic solid with practical applications and currently a very active research field, due to the fascinating properties associated with the coexistence of ferrous and ferric cations. Another important material by its structure, as well as by its applications in audio recording media, is maghemite or $\gamma\text{-Fe}_2\text{O}_3$, which can be considered as a defective spinel $\square_{1/3}\text{Fe}_{8/3}^{3+}\text{O}_4$, where \square represents vacancies on cation sites.

The overall symmetry of oxygens is fcc (face centered cubic), which defines two types of interstitial sites: 64 tetrahedral sites and 32 octahedral sites, for a unit cell containing 8 times the basic formula AB_2O_4 . Only one-eighth of tetrahedral sites and half of octahedral sites are occupied by cations. The space group is $\text{Fd}\bar{3}\text{m}$.

In MgAl_2O_4 , Al and Mg cations occupy the octahedral and tetrahedral sites, respectively. This cation distribution, known as a *normal* spinel, is usually indicated as

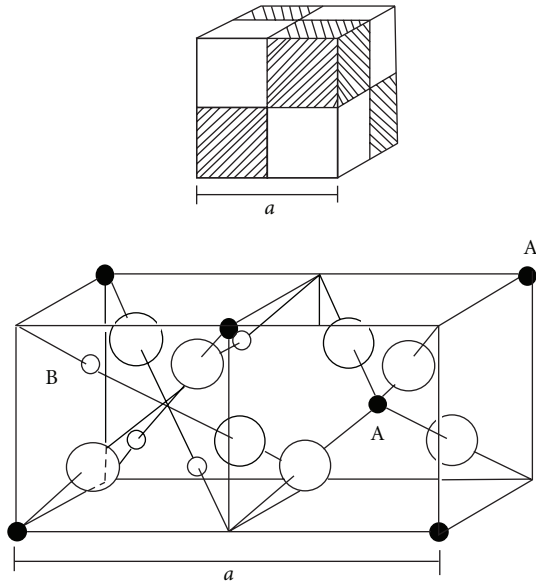


FIGURE 1: The unit cell of the spinel structure, divided into octants to show the tetrahedral (small, black spheres A) and octahedral (small white spheres B) sites. Oxygens are the large white spheres [1].

(Mg)[Al₂]O₄; that is, square brackets contain the octahedral sites occupancy (“B” sites), while parenthesis show the cations in tetrahedral sites (“A” sites). A radically different cation distribution, where half of trivalent cations (denoted by T³⁺) occupy A sites and B sites are shared by divalent cations (denoted by D²⁺) and the remaining trivalent cations (T³⁺)[T³⁺D²⁺]O₄, is known as the *inverse* spinel. An intermediate cation distribution can be expressed as (D_{1-δ}T_δ)[D_δT_{2-δ}]O₄, where δ is the degree of inversion. In many intermediate spinels, δ depends on the preparation technique and, more specifically, on the cooling rate after sintering or annealing.

A remarkable characteristic of spinel structure is that it is able to form an extremely wide variety of *total solid solutions*. This means that the composition of a given ferrite can be strongly modified, while the basic crystalline structure remains the same. An example is the Zn-Ni system, with general formula Zn_xNi_{1-x}Fe₂O₄, where 0 ≤ x ≤ 1. In the present example, the end compositions NiFe₂O₄ (for x = 0) and ZnFe₂O₄ (x = 1) can be obtained. NiFe₂O₄ is an inverse spinel: in contrast, ZnFe₂O₄ is a normal spinel. The properties of these compounds are very different: Ni ferrite is ferrimagnetic with a Curie temperature ≈ 858 K, while Zn ferrite is antiferromagnetic, with a Néel temperature about 9 K. This means that the general properties of the ferrite (as discussed in the following section) can be easily “tailored” just by varying the composition. Cations forming spinel solid solutions appear in Table 1.

The cation distribution in spinels was an interesting problem for some time; currently, it has been established that it depends essentially on various factors. First the *elastic energy* (the lattice deformation produced by cation radii differences) has to be considered. It refers to the degree of

TABLE 1: Some cations forming spinel solid solutions.

1+	2+	3+	4+
Li	Mg	Al	Ti
Cu	Ca	Ti	V
Ag	Mn	V	Mn
	Fe	Cr	Ge
	Co	Mn	Sn
	Ni	Fe	
	Cu	Ga	
	Zn	Rh	
	Cd	In	

From [1].

distortion of the crystal structure, as a result of differences in dimensions of the several cations within the specific spinel. In principle, small cations should occupy the smallest sites (tetrahedral sites), while larger cations should locate on the larger octahedral sites. However, trivalent cations are generally smaller than divalent ones, leading to some tendency to the inverse structure. The next factor to be considered is *electrostatic energy* (Madelung energy), which has to do with the electrical charge distribution. In a simple way, cations with high electrical charge should occupy the sites with larger coordination number (octahedral), and cations with smaller valency should be more stable when occupying the tetrahedral sites. The *crystal field* stabilization energy comes next to account for cation site “preference.” This energy has to do with the geometry of *d* orbitals and the arrangements these orbitals can established within the crystal structure. The five *d* orbitals no longer have the same energy but are split according to the electric field distribution established by anions on the particular crystal site. The physical basis for this differences in energy is simply the electrostatic repulsion between the *d* electrons and the orbitals of the surrounding *p* orbitals of anions.

Since bonding in most ferrites has an ionic character, cations are surrounded by anions, and conversely anions have cations as nearest neighbors. Magnetic ordering in ferrites (as in many oxides) tends to form antiferromagnetic arrangements, as interactions between cations have to be established through the anions. However, in most cases a resulting magnetic moment remains due to the fact that magnetic lattices contain different numbers of cations. In the case of spinels, the magnetic structure can be inferred from a small part of the structure, as shown in Figure 2 Superexchange interactions can then be schematized as a triangular arrangement. The strongest interactions are AOB, which occur between tetrahedral and octahedral cations, followed by BOB (cations on neighboring octahedral sites).

The relative strength of these interactions can be illustrated by the Curie temperature of Li and Zn ferrites (both Li and Zn are paramagnetic cations). Li_{0.5}Fe_{2.5}O₄ is an inverse spinel, with a cation distribution that can be expressed as Fe [Li_{0.5}Fe_{1.5}] O₄, while Zn ferrite is a normal spinel, (Zn)[Fe₂]O₄. Iron ions have an antiparallel order in both

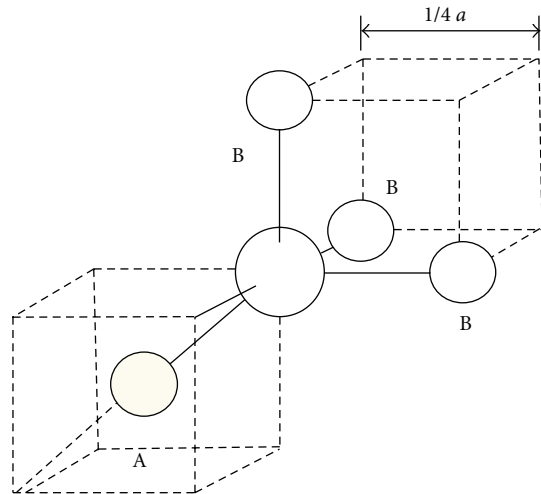


FIGURE 2: Detail of the A and B sites around an oxygen, to show AB and BB interactions.

ferrites, but as they both occupy octahedral sites, they compensate completely in Zn ferrite. In the case of Li ferrite, they have also an antiparallel order, but they belong to different sublattices, with different number. As a result, Zn ferrite is anti-ferromagnetic (with zero resulting magnetization), and Li ferrite is ferromagnetic, with a magnetization (per formula unit) of about 0.5 Bohr magneton (close to 0 K). The strength of interactions is apparent in the transition temperatures: the Curie point for Li ferrite is the highest observed in spinels 958 K, while Néel temperature for Zn ferrite is the lowest in spinels 9 K.

An interesting system is $\text{Zn}_x\text{Ni}_{1-x}\text{Fe}_2\text{O}_4$, which is normal for Zn and inverse for Ni. The general site occupancy can be expressed as: $(\text{Zn}_x\text{Fe}_{1-x})[\text{Ni}_{1-x}\text{Fe}_{1+x}]\text{O}_4$. The composition varies from Ni ferrite ($x = 0$) to Zn ferrite ($x = 1$). Starting with Ni ferrite, the decrease in x occurs as if Zn entering in A sites “push” Fe toward B sites, filling the octahedral sites left by the decreasing Ni ions. As in all inverse ferrites, the low-temperature global magnetization depends on the divalent cation (as Fe ions are antiparallel). The presence of Zn decreases the magnetization in A sublattice and increases the B sublattices. The addition of a paramagnetic cation thus leads to an increase in total magnetization! However, as Zn increases in A sites, AOB interaction weakens, and for $x \approx 0.65$, BOB interaction is comparable to AOB interaction leading to a triangular structure (known as Yafet-Kittel [3]).

The Curie temperature shows also a large variation with composition for ZnNi ferrites, $T_C = 858 \text{ K}$ for $x = 0$ (Ni ferrite), and as mentioned above, Zn ferrite is antiferromagnetic, with $T_N = 9 \text{ K}$.

2.2. Garnets. The crystal structure is that of the garnet mineral, $\text{Mn}_3\text{Al}_2\text{Si}_3\text{O}_{12}$. The magnetic garnets include Fe^{3+} instead of Al and Si, and a rare earth cation (R) substitutes Mn, to give the general formula $\text{R}_3\text{Fe}_5\text{O}_{12}$ for ferromagnetic garnets [4, 5]. The crystal structure has cubic symmetry and is relatively complex; the unit cell has 8 formula units (160 atoms) and belongs to the space group O_h^{10} -Ia3d. In

contrast with spinels, the oxygen sublattice is not a close-packed arrangement, but it is better described as a polyhedra combination. Three kinds of cation sites exist in this structure: dodecahedral (eightfold), octahedral (sixfold), and tetrahedral (fourfold) sites. Rare earth cations, R, occupy the largest, dodecahedral sites, while Fe^{3+} cations distribute among the tetra- and octahedral places. The cation distribution is generally expressed as $\{\text{R}_3\}(\text{Fe}_3)[\text{Fe}_2]\text{O}_{12}$; $\{\}$ bracket denotes dodecahedral sites, $()$ parenthesis are used for tetrahedral site occupancy, and octahedral sites are indicated by square brackets $[\]$. Rare earth cations (from La^{3+} to Lu^{3+}) enter the dodecahedral sites, and as spinels, garnets can form total solid solutions. A wide variety of cation substitutions has been reported [6]. Yttrium iron garnet, $\text{Y}_3\text{Fe}_5\text{O}_{12}$ also known as “YIG,” has remarkable magnetic properties.

The magnetic structure of garnets can be described by three magnetic sublattices, with a superexchange interaction through oxygens. Dodecahedral and octahedral ions are parallel, while tetrahedral cations adopt an antiparallel orientation. At very low temperatures, global magnetization (per formula unit) is roughly $(3\mu_R - \mu_{\text{Fe}})$, where μ_R and μ_{Fe} are the rare earth and the iron magnetic moments, respectively. The differences in thermal behavior among the three sublattices lead to the *compensation* of magnetic moments. As temperature increases, the magnetization in each sublattice is affected by the thermal agitation and decreases. This reduction in magnetization is slow in iron sublattices, but, due to its larger size, the decrease is quite steeply in the dodecahedral sublattice. At a certain temperature, the reduction in magnetization in rare earth sublattice exactly compensates the difference between octa- and tetrahedral sublattice, and global magnetization exhibits a zero value. For GdIG, this temperature is 300 K. The fact that magnetic structure is dominated by iron sublattices can also be observed in the Curie temperature: virtually all iron garnets show the same transition point ($\sim 560 \text{ K}$).

2.3. Hexaferrites. All of hexagonal ferrites are synthetic; barium hexaferrite ($\text{BaFe}_{12}\text{O}_{19}$) possesses the same structure as the natural mineral magnetoplumbite, of approximate formula $\text{PbFe}_{7.5}\text{Mn}_{3.5}\text{Al}_{0.5}\text{Ti}_{0.5}\text{O}_{19}$. Rather than sharing a common crystal structure, hexaferrites are a family of related compounds with hexagonal and rhombohedral symmetry. The main compositions can be represented in the upper section of the $\text{MeO}-\text{Fe}_2\text{O}_3-\text{BaO}$ ternary phase diagram. Me is a divalent cation such as Ni, Mg, Co, Fe, Zn, Cu, for instance. All the magnetic hexaferrites are found on the $\text{BaFe}_{12}\text{O}_{19}-\text{Me}_2\text{Fe}_4\text{O}_8$ and $\text{BaFe}_{12}\text{O}_{19}-\text{Me}_2\text{BaFe}_{12}\text{O}_{22}$ joins (Figure 3). If the end members are designated as M ($\text{BaFe}_{12}\text{O}_{19}$), S ($\text{Me}_2\text{Fe}_4\text{O}_8$), and Y ($\text{Me}_2\text{BaFe}_{12}\text{O}_{22}$); the joins are M-S and M-Y, respectively. Some of the main compositions are found in Table 2.

Hexaferrites can also form an extensive variety of solid solutions. Ba can be substituted by Sr, Ca, and Pb. Fe^{3+} can be substituted by trivalent cations such as Al, Ga, In, Sc [8], or by a combination of divalent + tetravalent cations, such as $\text{Co}^{2+} + \text{Ti}^{4+}$. A more complete account of these solid solutions can be found in [1].

TABLE 2: Formulae of some hexaferrites and their formation from end members of the ternary phase diagram.

Designation	Formula
M	$\text{BaFe}_{12}\text{O}_{19}$
Y	$\text{Ba}_2\text{Me}_2\text{Fe}_{12}\text{O}_{22}$
W (MS)	$\text{BaMe}_2\text{Fe}_{16}\text{O}_{27}$
X (M_2S)	$\text{Ba}_2\text{Me}_2\text{Fe}_{28}\text{O}_{46}$
U (M_2Y)	$\text{Ba}_4\text{Me}_2\text{Fe}_{36}\text{O}_{60}$
Z (M_2Y_2)	$\text{Ba}_6\text{Me}_4\text{Fe}_{48}\text{O}_{82}$

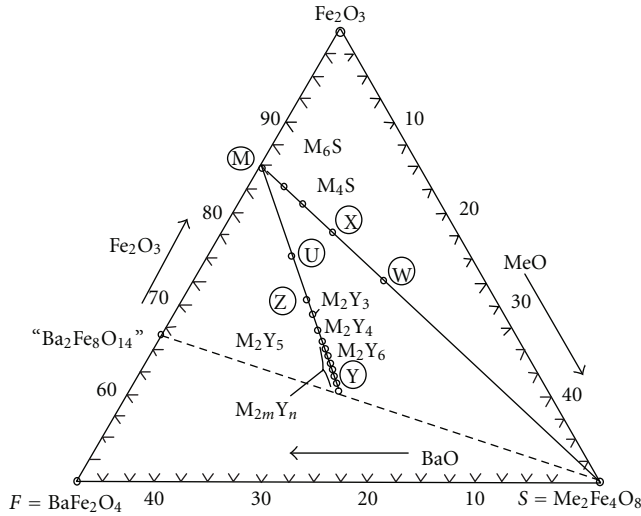


FIGURE 3: Upper triangle of the Fe_2O_3 -BaO-MeO phase diagram showing the several compositions of hexaferrites [7].

The magnetic structure in hexaferrites is complex, as a consequence of their complex crystal structure. In $\text{BaFe}_{12}\text{O}_{19}$, iron ions occupy five different sublattices, with a total magnetization $20\mu_B$ per formula unit, at low T . A detailed analysis of magnetic and crystal structures can be found in (9). The most interesting feature of hexaferrites is their high coercivity.

2.4. Preparation of Ferrites. Ferrites were first prepared by ceramic methods, involving milling, mixing, pressing, sintering, and finishing as basic operations, to obtain bulk materials with grains in the micrometric scale. However, as a result of the general current tendency to circuit integration and miniaturization, ferrites are prepared in the form of thick and thin films and, more recently, as nanostructured materials.

Ferrite thin films can be polycrystalline or epitaxial films. Major methods to obtain ferrite thin films are electroplating (or ferrite plating) [9], magnetron sputtering (single and multitarget) [10], pulsed laser deposition [11], and molecular beam epitaxy [12]. A detailed account of epitaxial ferrite films can be found in [13].

An additional route to tuning ferrite properties for specific applications is the production of heterostructures, that is,

the artificial layering of ferrites with isostructural and non-isostructural materials, such as $\text{Fe}_3\text{O}_4/\text{NiO}$ (53), $\text{Fe}_3\text{O}_4/\text{CoO}$ (56), and $(\text{Mn,Zn})\text{Fe}_2\text{O}_4/\text{Co Fe}_2\text{O}_4$ [14], and incorporating them into planar devices. The combination of ferrite layers with piezoelectric layers is leading to new and exciting applications, as reported below.

By reducing the scale to the nanometric size, new and technologically interesting properties have been obtained. Nanocrystalline magnetic materials have been obtained by a variety of methods, such as coprecipitation [15], hydrothermal [16], sonochemical [17], citrate precursor [18], sol-gel [19], mechanical alloying [20], shock wave [21], reverse micelle [22], forced hydrolysis in a polyol [23], and even by using egg white as an aqueous medium [24].

The preparation methods of ferrites for applications in biotechnology are reported below.

3. Novel Applications of Ferrites

3.1. Inductors. Ferrites are primarily used as inductive components in a large variety of electronic circuits such as low-noise amplifiers, filters, voltage-controlled oscillators, impedance matching networks, for instance. Their recent applications as inductors obey, among other tendencies, to the general trend of miniaturization and integration as ferrite multilayers for passive functional electronic devices. The multilayer technology has become a key technology for mass production of integrated devices; multilayers allow a high degree of integration density. Multilayer capacitors penetrated the market a few decades ago, while inductors started in the 1980s. The basic components to produce the inductance are a very soft ferrite and a metallic coil.

In addition, to provide a high permeability at the operation frequency, the ferrite film should be prepared by a process compatible with the integrated circuit manufacturing process. Sputtering provides films with high density, but the composition is sometimes difficult to control with accuracy, and the annealing processes can attain high temperatures. Pulsed laser deposition leads to high-quality films; however, a method involving the preparation of the ferrite film by a combination of sol-gel and spin-coating seems easier and with a lower cost [25].

Layered samples of ferrites with piezoelectric oxides can lead to a new generation of magnetic field sensors. The basis of their performance is the capability of converting magnetic fields into electrical voltages by a two-step process. First, the magnetic field produces a mechanical strain on the magnetic material (due to its magnetostriction); this strain then induces a voltage in the piezoelectric layer. These sensors can provide a high sensitivity, miniature size, and virtually zero power consumption. Sensors for ac and dc magnetic fields, ac and dc electric currents, can be fabricated. Sensors based on nickel ferrite ($\text{Ni}_{1-x}\text{Zn}_x\text{Fe}_2\text{O}_4$ with $x = 1-0.5$)/lead zirconate-titanate ($\text{PbZr}_{0.52}\text{Ti}_{0.48}\text{O}_3$) have shown an excellent performance [26]. Both ferrite and zirconate-titanate films are prepared by tape casting; typically, 11 ferrite layers were combined with 10 piezoelectric layers (both layers $18\mu\text{m}$ thick, $3 \times 6\text{ mm}^2$ area).

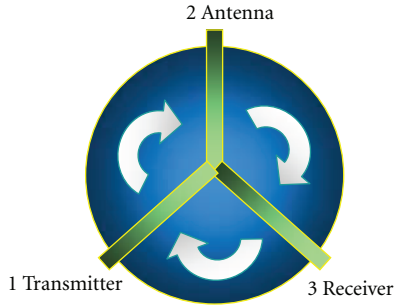


FIGURE 4: Schematic representation of a circulator.

3.2. High Frequency. There has been an increasing demand of magnetic materials for high-frequency applications such as telecommunications and radar systems, as microwave technology requires higher frequencies and bandwidths up to 100 GHz. Ferrites are nonconducting oxides and therefore allow total penetration of electromagnetic fields, in contrast with metals, where the skin effect severely limits the penetration of high-frequency fields [27]. At such frequencies, domain walls are unable to follow the fields (dispersion of domain walls typically occurs about 10 GHz), and absorption of microwave power takes place by spin dynamics. The usual geometry is to align spins first with a DC magnetic field H and apply the microwave field perpendicular to H . The spins precess around their equilibrium orientation at the frequency of the microwave field. The classical description of this dynamics is the Landau-Lifshitz equation [28] of motion, which can be written in its undamped form:

$$\frac{dM}{dt} = \gamma M \times H_i, \quad (1)$$

where M is the magnetization, γ is the gyromagnetic ratio (ratio of mechanical to magnetic moment, $\gamma = ge/2mc = 2.8 \text{ MHz/G}$), and H_i is the total internal field acting upon the spin. The magnetization and the field terms can be separated in the static and time-dependent parts as

$$H = H_i + h e^{i\omega t}, \quad M = M_s + m e^{i\omega t} \quad (2)$$

These equations show a singularity at

$$\omega = \omega_0 = \gamma H_0 \quad (3)$$

H_0 is the total field on the spins (external and internal); (3) expresses the ferromagnetic resonance (FMR) conditions and is known as the Larmor equation. FMR is associated with the uniform (in phase) precession of spins. The upper limit of applications of ferrites is FMR, since the interaction with the microwave field becomes negligible as $\omega > \omega_0$. Spinel are therefore applied at frequencies up to 30 GHz, while this limit is about 10 GHz for garnets and can attain 100 GHz for hexaferrites.

The absorption of microwaves by ferrites involves losses; a damping or relaxation term is normally added to (3). In polycrystalline ferrites, losses are associated with defects and the anisotropy field distribution, and with electrical conduction a common problem, especially in spinels, is the presence

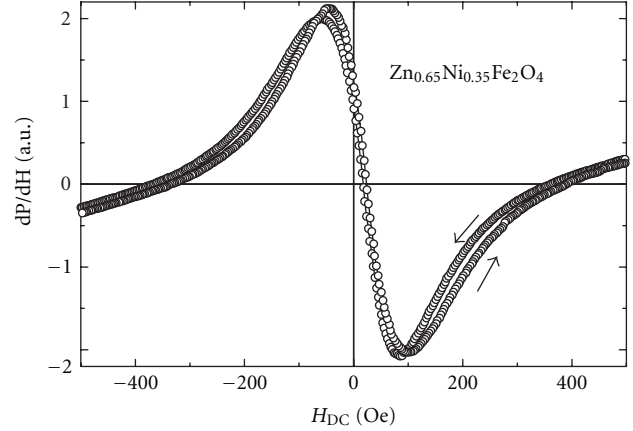


FIGURE 5: Low-field microwave absorption (LFA) of a Ni-Zn ferrite at 9.4 GHz room temperature and room temperature. A small hysteresis is observed for increasing and decreasing applied field.

of Fe^{2+} , which promotes a hopping conduction process in combination with Fe^{3+} . The physical origin of losses in polycrystalline ferrites, through its effects on the linewidth, has been recently investigated in detail; the dominant role of grain boundaries is apparent [29, 30].

Some of ferrite applications rely on the fact that the spin rotation depends on the orientation of the external field, which allows the control of the interaction with the microwave field. For one direction of the field, the ferrite transmits the microwave field; for the opposite, it strongly absorbs it. This is the basis of nonreciprocal devices.

Typical devices are circulators, isolators, phase shifters, and antennas. Circulators were developed for radar systems and are now used in mobile phones. They allow the use of the same device for transmission and reception of the response signal. As shown schematically in Figure 4, any signal entering through port 1 exits by port 2, with no connection with port 3. If the generator is connected to port 1 and the antenna to port 2, this is the path of the outgoing signal. The incoming signal enters through port 2 (the antenna) and is directed to port 3, to the receiver. This allows the handling of a strong outgoing signal (ports 1-2) together with a very sensitive detector (ports 2-3), with no risk of damaging the receiver and using the same antenna. Circulators are usually fabricated with garnets.

Recently, a nonresonant absorption of microwave power at very low magnetic fields has been receiving attention. This absorption, known as LFA (for low-field microwave Absorption), has shown to be clearly dominated by the anisotropy field, H_K , of the ferro- or ferrimagnetic material [31]. Recent results obtained in a Ni-Zn ferrite are shown in Figure 5 in many respects, this absorption is similar to giant magnetoimpedance, GMI [32], that is, the change in electric impedance of a material when subjected to a DC magnetic field [33]. A significant difference with GMI is that LFA does not need that the electrical conductivity of the sample be

of metallic type. No practical applications of LFA have been proposed, so far; however, it is possible to expect that similar applications to GMI can be made (sensors for magnetic field, DC electric current, mechanical stress, etc.), with the additional advantages over classic GMI of high frequencies and insulator magnetic materials.

3.3. Power. Power applications of ferrites are dominated by the power supplies for a large variety of devices such as computers, all kinds of peripherals, TV and video systems, and all types of small and medium instruments. The main application is in the systems known as switched-mode power supplies (SMPSs). In this application, the mains power signal is first rectified it is then switched as regular pulses (typically rectangular) at a high frequency to feed into a ferrite transformer, and finally it is rectified again to provide the required power to the instrument. An increase in power delivery and efficiency can be obtained by increasing the working frequency of the transformer.

A recent approach to increase efficiency of the ferrite cores is based on the decrease of eddy currents, by increasing resistivity. Beside the use of nonconducting additives that locate preferentially on grain boundaries (and limit the intergrain conductivity), MnZn and NiZn are combined as $\text{Mn}_x\text{Ni}_{0.5-x}\text{Zn}_{0.5}\text{Fe}_2\text{O}_4$ and obtained through a citrate precursor method [34].

An additional difficulty appears in the case of power applications at high temperature, as is the case of some automotive power devices. Due to the closeness to the car engine, the working temperature increases from the usual 80–100°C for standard applications, to 140°C. A proposed solution involves the modification of the MnZn ferrites (used previously for these applications) in order to produce a higher fraction of Fe^{2+} [35], such as $(\text{Mn}_{0.76}\text{Zn}_{0.17}\text{Fe}_{0.07}^{2+})\text{Fe}_2\text{O}_4$. This ferrous concentration presents a minimum in the magnetocrystalline anisotropy close to 140°C, and therefore, a minimum in losses appears at this temperature. The change is obtained through a careful control of the oxidation atmosphere during sintering and cooling.

As in all other applications, a strong need for miniaturization has also marked the developments in this area in the last few years. In addition to standard methods to obtain ferrite thin films (such as sputtering, laser ablation, sol-gel), screen or stencil printed ceramic-polymer composites have been investigated [36], combining the remarkable magnetic properties of ferrites with the processability of polymer thick films. These polymer thick films can be cured at temperatures about 200°C or less, leaving only the polymer binder and the ferrite filler. This technique allows the fabrication of highly integrated power circuits. The coil is obtained by patterning copper on a flexible polyimide substrate; the ferrite-polymer composite film is then printed above and below the plane of the coil. The magnetic ceramic filler is formed by MnZn ferrite particles about 10 μm , obtained by a standard method. The inductance value remains stable up to 124 MHz.

A different method based on a batch-fabrication method of 3D transformers and inductors has also been proposed [37]. The magnetic core is made of two half magnetic pieces and a printed circuit board (or flexi foil) carrying the

electric windings around the core. The 3D ferrite cores are microstructured out of a 1 mm thick ferrite wafer using a newly developed batch-type micropowder blasting process [38]. These transformers are well suited for low-power applications at working frequencies up to 1 MHz.

Losses in ferrites depend essentially on hysteresis loss at low frequencies, conductivity (or eddy current) loss, and relaxation-resonance loss at high frequencies; their modeling is complex. A model based on the Preisach theory [39] has been applied to predict the hysteretic behavior of soft ferrites for applications in power electronics [40], with good results at low frequencies. On the other hand, by using a network model based on the total energy loss (not only hysteresis loss), a good agreement with experimental results for power, signal, and electromagnetic interference has been found [41]. The approach offers a mechanism for the inclusion of parameters such as temperature or stress variations.

3.4. Electromagnetic Interference (EMI) Suppression. The significant increase in the amount of electronic equipment such as high-speed digital interfaces in notebooks and computers, digital cameras, scanners, and so forth, in small areas, has seriously enhanced the possibility of disturbing each other by electromagnetic interference (EMI). In particular, the fast development of wireless communications has led to interference induced by electric and magnetic fields. Electromagnetic interference can be defined as the degradation in performance of an electronic system caused by an electromagnetic disturbance [42]. The noise from electric devices is usually produced at frequencies higher than circuit signals. To avoid, or at least reduce EMI, suppressors should work as low-pass filters, that is, circuits that block signals with frequencies higher than a given frequency value.

There are several approaches to build EMI suppressors: soft ferrites [43], ferromagnetic metals [44], ferromagnetic metal/hexaferrite composites [45], encapsulated magnetic particles [46], and carbon nanotube composites [47].

Ferrite components for EMI suppressors have been used for decades. In the recent years, however, there have been special needs for these materials as a consequence of the miniaturization trends, increase in integration density, and increase in higher clock frequency, especially in communication, computing, and information technologies. Ferrite multilayer components have been developed as a response to these needs, formed essentially by a highly conductive layer embedded in a ferrite monolithic structure, produced by ceramic coprocessing technologies. Typically, Ni-Zn ferrites are used for the 20–200 MHz frequency range. Multilayer suppressors behave like a frequency-dependent resistor; at low frequencies, losses in the ferrite are negligible. As frequency increases, losses increase also, and, as ferromagnetic resonance is approached, the inductor behaves as a frequency-independent resistor and no longer as an inductor.

Hexaferrites represent an interesting alternative to cubic ferrites as EMI suppressor components; they possess higher resonance frequencies, relatively high permeabilities (at microwave frequencies), and high electrical resistivities. Metallic ferromagnets, in contrast, show a larger saturation

magnetization, but, as frequency increases, they exhibit a strong decrease in permeability due to eddy currents. However, in combination with hexaferrites, they have shown a strong potential for EMI suppressor devices [45]. Co_2Z and Zn_2Y hexaferrite particles ($10\text{--}30\text{ }\mu\text{m}$), mixed with metallic Ni particles ($2\text{--}3\text{ }\mu\text{m}$), and prepared with a polymer (polyvinylidene fluoride) by hot pressing at low temperature led to high shield effectiveness.

Carbon nanotube-polystyrene foam composites have shown a high EMI shielding effectiveness based on a mechanism associated with the reflection of electromagnetic radiation [48]; no magnetic material is used.

Ferrite nanoparticles in combination with carbon nanotubes can efficiently absorb microwave radiation. Carbon nanotubes/ CoFe_2O_4 spinel nanocomposite was fabricated by a chemical vapor deposition method using CoFe_2O_4 nanoparticles as catalysts [46]. The microwave absorption ($2\text{--}18\text{ GHz}$ range) was enhanced. For carbon nanotubes, dielectric loss contributes to the energy loss of electromagnetic waves, while, for pure Co ferrite, the effects of microwave absorption are associated with magnetic losses, but both isolated mechanisms are poor absorbers. For the nanocomposites, however, the microwave absorption improves because of a better match between the dielectric loss and the magnetic loss, which originates from the combination of paramagnetic nanotubes and ferromagnetic material. The dispersed CoFe_2O_4 nanoparticles absorb the microwave signals by resonance effects due to shape anisotropy and dipolar interactions between particles. Such effects are weakened in congregated particles.

3.5. Biosciences. Magnetic materials in the form of nanoparticles, mainly magnetite (Fe_3O_4), are present in various living organisms [49] and can be used in a number of applications. Magnetic nanoparticles can, of course, be prepared in the laboratory by means of the well-known methods; however, magnetic biogenic particles have better properties than synthetic ones: they have a definite size range and width/length ratio and high chemical purity, they are almost perfect crystallographically, and sometimes they possess unusual crystallographic morphologies. Extracellular production of nanometer magnetite particles by various types of bacteria has been described [50]. In many cases, the biogenic particles retain a lipid layer which makes them very stable and easily biocompatible.

Many biotechnological applications have been developed based on biogenic and synthetic magnetic micro- and nanoparticles [51]. Magnetic nanoparticles have been used to guide radionuclides to specific tissues. An approach has been developed to directly label a radioisotope with ferrite particles [52] in *in vivo* liver tissue in rats. Therapeutic applications are feasible by further conjugation with other medicals.

In magnetic resonance imaging (MRI), magnetite superparamagnetic particles are selectively associated with healthy regions of some tissues (liver, for instance); since these particles change the rate of proton decay from the excited to the ground state (which is the basis of MRI), a different, dark-

er contrast is obtained from these healthy regions of tissue [53, 54].

Thermal energy from hysteresis loss of ferrites can be used in hyperthermia, that is, the heating of specific tissues or organs for treatment of cancer. The temperature in tumor tissues rises and becomes more sensitive to radio- or chemotherapy. In addition of magnetite [55], several spinel ferrites (M-Zn , with $\text{M} = \text{Mn, Co, Fe}^{2+}$, and $\text{Fe}^{2+}\text{--Mn}$) are under investigation [56] as well as hexaferrites [57].

Enzymes, oligonucleotides, antibodies, and other biologically active compounds can be immobilized, as an important technique used in biotechnology. Such immobilized compounds can be targeted to a specific place or can be removed from the system by using an external magnetic field. The compounds can exert their activity on the specific place or tissue or can be used as affinity ligands to trap the cells or target molecules [58].

Magnetic nanoparticles can also be used in a variety of applications: modification, detection, isolation, and study of cells [59], and isolation of biologically active compounds [60], for instance.

4. Conclusions

Ferrites have been studied and applied for more than 50 years and are considered as well-known materials with “mature” technologies ranging from hard magnets to magnetic recording and to microwave devices. However, the advances in applications and fabrication technologies in the last 10 years have been impressive. Bulk ferrites remain a key group of magnetic materials, while nanostructured ferrites show a dramatic promise for applications in even significantly wider fields.

References

- [1] R. Valenzuela, *Magnetic Ceramics*, Cambridge University Press, 2005.
- [2] W. H. Bragg, “The structure of the spinel group of crystals,” *Philosophical Magazine*, vol. 30, no. 176, pp. 305–315, 1915.
- [3] Y. Yafet and C. Kittel, “Antiferromagnetic arrangements in ferrites,” *Physical Review*, vol. 87, no. 2, pp. 290–294, 1952.
- [4] F. Bertaut and F. Forrat, “Structure des ferrites ferrimagnétiques des terres rares,” *Comptes Rendus de l’Académie des Sciences*, vol. 242, pp. 382–384, 1956.
- [5] S. Geller and M. A. Gilleo, “The crystal structure and ferrimagnetism of yttrium-iron garnet, $\text{Y}_3\text{Fe}_2(\text{FeO}_4)_3$,” *Journal of Physics and Chemistry of Solids*, vol. 3, no. 1-2, pp. 30–36, 1957.
- [6] M. A. Gilleo, “Ferromagnetic Insulators: garnets,” in *Ferromagnetic Materials*, E. R. Wohlfarth, Ed., vol. 2, North Holland, The Netherlands, 1980.
- [7] G. Wrinkler, “Crystallography, chemistry and technology of ferrites,” in *Magnetic Properties of Materials*, J. Smit, Ed., p. 20, McGraw-Hill, London, UK, 1971.
- [8] G. Albanese, M. Carbuicchio, and A. Deriu, “Substitution of Fe^{3+} by Al^{3+} in the trigonal sites of M-type hexagonal ferrites,” *Il Nuovo Cimento B*, vol. 15, no. 2, pp. 147–158, 1973.
- [9] M. Abe, Y. Kitamoto, K. Matsumoto, M. Zhang, and P. Li, “Ultrasound enhanced ferrite plating; bringing breakthrough in ferrite coating synthesized from aqueous solution,” *IEEE Transactions on Magnetics*, vol. 33, no. 5, pp. 3649–3651, 1997.

- [10] J. J. Cuomo, R. J. Gambino, J. M. E. Harper, J. D. Kuptsis, and J. C. Webber, "Significance of negative ion formation in sputtering and sims analysis," *Journal of Vacuum Science & Technology*, vol. 15, no. 2, pp. 281–287, 1978.
- [11] D. Dijkkamp, T. Venkatesan, X. D. Wu et al., "Preparation of Y-Ba-Cu oxide superconductor thin films using pulsed laser evaporation from high T_c bulk material," *Applied Physics Letters*, vol. 51, no. 8, pp. 619–621, 1987.
- [12] D. M. Lind, S. D. Berry, G. Chern, H. Mathias, and L. R. Testardi, "Growth and structural characterization of Fe₃O₄ and NiO thin films and superlattices grown by oxygen-plasma-assisted molecular-beam epitaxy," *Physical Review B*, vol. 45, no. 4, pp. 1838–1850, 1992.
- [13] Y. Suzuki, "Epitaxial spinel ferrite thin films," *Annual Review of Materials Science*, vol. 31, pp. 265–289, 2001.
- [14] Y. Suzuki, R. B. Van Dover, E. M. Gyorgy, J. M. Phillips, and R. J. Felder, "Exchange coupling in single-crystalline spinel-structure (Mn,Zn)Fe₂O₄/CoFe₂O₄ bilayers," *Physical Review B*, vol. 53, no. 21, pp. 14016–14019, 1996.
- [15] J. M. Yang, W. J. Tsuo, and F. S. Yen, "Preparation of ultrafine nickel ferrite powders using mixed Ni and Fe tartrates," *Journal of Solid State Chemistry*, vol. 145, no. 1, pp. 50–57, 1999.
- [16] J. Zhou, J. Ma, C. Sun et al., "Low-temperature synthesis of NiFe₂O₄ by a hydrothermal method," *Journal of the American Ceramic Society*, vol. 88, no. 12, pp. 3535–3537, 2005.
- [17] K. V. P. M. Shafi, Y. Koltypin, A. Gedanken et al., "Sonochemical preparation of nanosized amorphous NiFe₂O₄ particles," *Journal of Physical Chemistry B*, vol. 101, no. 33, pp. 6409–6414, 1997.
- [18] S. Prasad and N. S. Gajbhiye, "Magnetic studies of nanosized nickel ferrite particles synthesized by the citrate precursor technique," *Journal of Alloys and Compounds*, vol. 265, no. 1–2, pp. 87–92, 1998.
- [19] D. -H. Chen and X. -R. He, "Synthesis of nickel ferrite nanoparticles by sol-gel method," *Materials Research Bulletin*, vol. 36, no. 7–8, pp. 1369–1377, 2001.
- [20] Y. Shi, J. Ding, X. Liu, and J. Wang, "NiFe₂O₄ ultrafine particles prepared by co-precipitation/mechanical alloying," *Journal of Magnetism and Magnetic Materials*, vol. 205, no. 2, pp. 249–254, 1999.
- [21] J. Liu, H. He, X. Jin, Z. Hao, and Z. Hu, "Synthesis of nanosized nickel ferrites by shock waves and their magnetic properties," *Materials Research Bulletin*, vol. 36, no. 13–14, pp. 2357–2363, 2001.
- [22] A. Kale, S. Gubbala, and R. D. K. Misra, "Magnetic behavior of nanocrystalline nickel ferrite synthesized by the reverse micelle technique," *Journal of Magnetism and Magnetic Materials*, vol. 277, no. 3, pp. 350–358, 2004.
- [23] Z. Beji, T. Ben Chaabane, L. S. Smiri et al., "Synthesis of nickel-zinc ferrite nanoparticles in polyol: morphological, structural and magnetic studies," *Physica Status Solidi A*, vol. 203, no. 3, pp. 504–512, 2006.
- [24] S. Maensiri, C. Masingboon, B. Boonchom, and S. Seraphin, "A simple route to synthesize nickel ferrite (NiFe₂O₄) nanoparticles using egg white," *Scripta Materialia*, vol. 56, no. 9, pp. 797–800, 2007.
- [25] C. Yang, F. Liu, T. Ren et al., "Fully integrated ferrite-based inductors for RF ICs," *Sensors and Actuators A*, vol. 130–131, pp. 365–370, 2006.
- [26] Y. K. Fetisov, A. A. Bush, K. E. Kamentsev, A. Y. Ostashchenko, and G. Srinivasan, "Ferrite-piezoelectric multilayers for magnetic field sensors," *IEEE Sensors Journal*, vol. 6, no. 4, Article ID 1661574, pp. 935–938, 2006.
- [27] M. Pardavi-Horvath, "Microwave applications of soft ferrites," *Journal of Magnetism and Magnetic Materials*, vol. 215, pp. 171–183, 2000.
- [28] L. D. Landau and E. Lifshitz, "On the theory of the dispersion of magnetic permeability in ferromagnetic bodies," *Physik Z. Sowjetunion*, vol. 8, pp. 153–169, 1935.
- [29] N. Mo, Y. Y. Song, and C. E. Patton, "High-field microwave effective linewidth in polycrystalline ferrites: physical origins and intrinsic limits," *Journal of Applied Physics*, vol. 97, no. 9, Article ID 093901, pp. 1–9, 2005.
- [30] N. Mo, J. J. Green, P. Krivosik, and C. E. Patton, "The low field microwave effective linewidth in polycrystalline ferrites," *Journal of Applied Physics*, vol. 101, no. 2, Article ID 023914, 2007.
- [31] R. Valenzuela, R. Zamorano, G. Alvarez, M. P. Gutiérrez, and H. Montiel, "Magnetoimpedance, ferromagnetic resonance, and low field microwave absorption in amorphous ferromagnets," *Journal of Non-Crystalline Solids*, vol. 353, no. 8–10, pp. 768–772, 2007.
- [32] H. Montiel, G. Alvarez, I. Betancourt, R. Zamorano, and R. Valenzuela, "Correlations between low-field microwave absorption and magnetoimpedance in Co-based amorphous ribbons," *Applied Physics Letters*, vol. 86, no. 7, Article ID 072503, pp. 1–3, 2005.
- [33] M. Knobel, M. Vazquez, and L. Kraus, "Giant Magnetoimpedance," in *Handbook of Magnetic Materials*, K. H. J. Buschow, Ed., vol. 15, p. 497, Elsevier Science, 2003.
- [34] A. Verma, M. I. Alam, R. Chatterjee, T. C. Goel, and R. G. Mendiratta, "Development of a new soft ferrite core for power applications," *Journal of Magnetism and Magnetic Materials*, vol. 300, no. 2, pp. 500–505, 2006.
- [35] V. Zaspalis, V. Tsakaloudi, E. Papazoglou, M. Kolenbrander, R. Guenther, and P. V. D. Valk, "Development of a new MnZn-ferrite soft magnetic material for high temperature power applications," *Journal of Electroceramics*, vol. 13, no. 1–3, pp. 585–591, 2004.
- [36] E. J. Brandon, E. E. Wesseling, V. Chang, and W. B. Kuhn, "Printed microinductors on flexible substrates for power applications," *IEEE Transactions on Components and Packaging Technologies*, vol. 26, no. 3, pp. 517–523, 2003.
- [37] F. Amalou, E. L. Bornand, and M. A. M. Gijs, "Batch-type millimeter-size transformers for miniaturized power applications," *IEEE Transactions on Magnetics*, vol. 37, no. 4, pp. 2999–3003, 2001.
- [38] E. Belloy, S. Thurre, E. Walckiers, A. Sayah, and M. A. M. Gijs, "Introduction of powder blasting for sensor and microsystem applications," *Sensors and Actuators. A*, vol. 84, no. 3, pp. 330–337, 2000.
- [39] F. Preisach, "Über die magnetische Nachwirkung," *Zeitschrift für Physik*, vol. 94, no. 5–6, pp. 277–302, 1935.
- [40] M. Angeli, E. Cardelli, and E. Della Torre, "Modelling of magnetic cores for power electronics applications," *Physica B*, vol. 275, no. 1–3, pp. 154–158, 2000.
- [41] P. R. Wilson, J. N. Ross, and A. D. Brown, "Modeling frequency-dependent losses in ferrite cores," *IEEE Transactions on Magnetics*, vol. 40, no. 3, pp. 1537–1541, 2004.
- [42] G. Stojanovic, M. Damnjanovic, V. Desnica et al., "High-performance zig-zag and meander inductors embedded in ferrite material," *Journal of Magnetism and Magnetic Materials*, vol. 297, no. 2, pp. 76–83, 2006.
- [43] Z. W. Li, L. Guoqing, L. Chen, W. Yuping, and C. K. Ong, "Co²⁺Ti⁴⁺ substituted Z-type barium ferrite with enhanced imaginary permeability and resonance frequency," *Journal of Applied Physics*, vol. 99, no. 6, Article ID 063905, 2006.

- [44] Y. B. Feng, T. Qiu, C. Y. Shen, and X. -Y. Li, "Electromagnetic and absorption properties of carbonyl iron/rubber radar absorbing materials," *IEEE Transactions on Magnetics*, vol. 42, no. 3, pp. 363–368, 2006.
- [45] B. W. Li, Y. Shen, Z.-X. Yue, and C.-W. Nan, "Enhanced microwave absorption in nickel/hexagonal-ferrite/polymer composites," *Applied Physics Letters*, vol. 89, no. 13, Article ID 132504, 2006.
- [46] R. C. Che, C. Y. Zhi, C. Y. Liang, and X. G. Zhou, "Fabrication and microwave absorption of carbon nanotubes CoFe_2O_4 spinel nanocomposite," *Applied Physics Letters*, vol. 88, no. 3, Article ID 033105, pp. 1–3, 2006.
- [47] C. Xiang, Y. Pan, X. Liu, X. Sun, X. Shi, and J. Guo, "Microwave attenuation of multiwalled carbon nanotube-fused silica composites," *Applied Physics Letters*, vol. 87, no. 12, Article ID 123103, pp. 1–3, 2005.
- [48] Y. Yang, M. C. Gupta, K. L. Dudley, and R. W. Lawrence, "Novel carbon nanotube—Polystyrene foam composites for electromagnetic interference shielding," *Nano Letters*, vol. 5, no. 11, pp. 2131–2134, 2005.
- [49] H. A. Lowenstam, "Magnetite in denticle capping in recent chitons (Polyplacophora)," *Bulletin Geological Society of America*, vol. 73, no. 4, pp. 435–438, 1962.
- [50] C. Zhang, H. Vali, C. S. Romaner, T. J. Phelps, and S. V. Liu, "Formation of single-domain magnetite by a thermophilic bacterium," *American Mineralogist*, vol. 83, no. 11-12, pp. 1409–1418, 1998.
- [51] I. Šafařík and M. Šafaříková, "Magnetic nanoparticles and biosciences," *Monatshefte für Chemie*, vol. 133, no. 6, pp. 737–759, 2002.
- [52] C. M. Fu, Y. F. Wang, Y. F. Guo, T. Y. Lin, and J. S. Chiu, "In vivo bio-distribution of intravenously injected Tc-99 m labeled ferrite nanoparticles bounded with biocompatible medicals," *IEEE Transactions on Magnetics*, vol. 41, no. 10, pp. 4120–4122, 2005.
- [53] C. R. Martin and D. T. Mitchell, "Nanomaterials in analytical chemistry," *Analytical Chemistry*, vol. 70, no. 9, pp. 322A–327A, 1998.
- [54] T. C. Yeh, W. Zhang, S. T. Ildstad, and C. Ho, "In vivo dynamic MRI tracking of rat T-cells labeled with superparamagnetic iron-oxide particles," *Magnetic Resonance in Medicine*, vol. 33, no. 2, pp. 200–208, 1995.
- [55] A. Jordan, R. Scholz, K. Maier-Hauff et al., "Presentation of a new magnetic field therapy system for the treatment of human solid tumors with magnetic fluid hyperthermia," *Journal of Magnetism and Magnetic Materials*, vol. 225, no. 1-2, pp. 118–126, 2001.
- [56] J. Giri, P. Pradhan, T. Sriharsha, and D. Bahadur, "Preparation and investigation of potentiality of different soft ferrites for hyperthermia applications," *Journal of Applied Physics*, vol. 97, no. 10, Article ID 10Q916, pp. 1–3, 2005.
- [57] D. H. Kim, S. H. Lee, K. N. Kim, K. M. Kim, I. B. Shim, and Y. K. Lee, "Temperature change of various ferrite particles with alternating magnetic field for hyperthermic application," *Journal of Magnetism and Magnetic Materials*, vol. 293, no. 1, pp. 320–327, 2005.
- [58] T. Matsunaga and S. Kamiya, "Use of magnetic particles isolated from magnetotactic bacteria for enzyme immobilization," *Applied Microbiology and Biotechnology*, vol. 26, no. 4, pp. 328–332, 1987.
- [59] I. Šafařík and M. Šafaříková, "Use of magnetic techniques for the isolation of cells," *Journal of Chromatography B*, vol. 722, no. 1-2, pp. 33–53, 1999.
- [60] K. Sode, S. Kudo, T. Sakaguchi, N. Nakamura, and T. Matsunaga, "Application of bacterial magnetic particles for highly selective mRNA recovery system," *Biotechnology Techniques*, vol. 7, no. 9, pp. 688–694, 1993.

